

Visible Light Induced Selective Photocatalytic Oxidation of Benzyl Amine to N-benzylidene-1-phenylmethanamine by Reduced Graphene Oxide-Titania Nanocomposites.

Soumya Gopi¹, Mothi Krishna Mohan^{1,2}, Honey Mary Joseph¹, S. Sugunan¹

¹Department of Applied Chemistry, Cochin University of Science and Technology,
Cochin-22, Kerala, India

²Christ University, Hosur Road, Bangalore 560029, Karnataka

Abstract

Irradiated semiconductor catalysis in the presence of molecular oxygen can be considered as an innovative and sustainable technique for organic transformations. The present work reports the preparation of Graphene oxide/TiO₂ composite by improved Hummer's method followed by hydrothermal technique. The prepared system was characterized by various physico-chemical techniques such as X-Ray diffraction, IR-Spectroscopy, UV-DRS, XPS, SEM and TEM Analysis. On reaction, benzylamine in CH₃CN yielded N-benzylidene-1-phenylmethanamine as the sole product. The reaction was monitored by GC-MS Analysis.

Keywords: Photo-oxidation, nanocomposites, TiO₂, Graphene, Benzylamine

I. Introduction

Semiconductor photocatalysis utilizing solar energy is a highly potential process for the production of materials, environmental purification and energy production. Photocatalysts are able to convert solar energy to chemical energy in order to oxidize or reduce materials (1,2). Heterogeneous photocatalysis has also been studied in selective organic transformations even though its application is limited due to nonselective nature (3-6). Photocatalytic reactions require only mild reaction conditions and are selective in radiation absorption (7). The sun delivers about 3×10^{24} J of energy to the earth's surface per year, which is about 4 orders of magnitude larger than the energy annually used by humans all over the world. Besides its abundance, solar energy is also clean and safe (8). Large number of semiconductor materials have been employed as photocatalysts but titanium dioxide (TiO₂) and its related materials are known to be the most reliable materials, because they are low-cost, stable under photo irradiation and exhibits high catalytic activity (9,10). TiO₂ has been widely used in many areas such as environmental remediation, self-cleaning surfaces, DSSC, water splitting etc. (11,12). TiO₂ crystallizes in three allotropic forms namely anatase, rutile and brookite out of which anatase is considered photocatalytically more active. Due to its large band gap (3.2 eV), the spectral response is limited in the UV region which constitutes only 4-5 % of the sun light. Varieties of strategies have been employed to improve the photocatalytic efficiency such as dye-sensitization, doping, coupling with different band gap semiconductors and loading with transition

metals (13-15). Among different TiO₂ composites, carbon materials have gained special attention because of its chemical inertness, stability, tuneable textural and chemical properties. Recently, nanostructured carbon materials (carbon nanotubes, fullerenes, graphene nanosheets) have studied in this context and among them graphene has emerged as one of the most important materials for the design of visible light responsive photocatalysts (16).

Graphene nanosheet exhibits properties such as superior electrical conductivity, excellent mechanical flexibility, large surface area, and high thermal/chemical stabilities (17-19). Graphene has the power to slow down the recombination of photo- or electro-chemically generated electron-hole pairs, increase the charge transfer rate of electrons and enhance the surface adsorption of chemical molecules through π - π interactions (20). Such graphene-based materials show unique electronic and optical properties and good biocompatibility, which make these materials attractive for many applications including energy storage, catalysis, biosensors, molecular imaging and drug delivery. Recently, graphene-based semiconductor photocatalysts have attracted much attention due to their good electron conductivity, large specific surface area and high adsorption ability (21).

Many efforts have been made for TiO₂ mediated organic redox-transformation for the last few years since it requires room temperature synthesis with O₂ under solar light irradiation. But most of these reactions were carried out under UV irradiation and the selectivity was also marginal (22-24). Here we

have prepared reduced graphene oxide-titanianano composite and the catalytic activity was checked in the photo-oxidation of benzylamine. By using our system, we were able to convert benzylamine to N-benzylidene-1-phenylmethanamine selectively. Photo-oxidation of these composite is known, but we are the first to report this particular oxidation at time duration of half an hour without the addition of molecular oxygen externally. Titania system with 5% reduced graphene oxide showed better photocatalytic activity in the degradation reaction using visible light and that is why the entire photo reaction was conducted using 5% graphene modified titania nanocomposite.

II. Experimental

2.1 Materials and Methods

Titanium(IV) isopropoxide was purchased from Sigma Aldrich, Germany. Graphite powder, KMnO_4 , benzyl amine and all the solvents were purchased from Merck Pvt. Ltd. India and used without any further purification. Structure, crystalline nature, phase purity, lattice parameters and impurity defects of the catalyst was identified by X-ray diffraction analysis. The powder X-ray diffraction of the sample was performed using a Bruker AXS D8 diffractometer with Ni filtered $\text{Cu K}\alpha$ radiation source ($k = 1.5406 \text{ \AA}$) in the range of $10\text{--}70^\circ$ at a scan rate of $0.5^\circ/\text{min}$. Light response of the catalysts were recorded in the range of $200\text{--}900 \text{ nm}$ on Labomed UV-Vis double beam UVD-500 spectrophotometer with a CCD detector, using BaSO_4 as reflectance standard. SEM was used to understand the morphology of the sample. SEM micrographs were taken using JEOL Model JSM- 6390LV with a resolution of 1.38 eV . Functional groups and titania based stretching vibrations were observed from Thermo NICOLET FT-IR instrument. Surface composition and electronic structures were analyzed by X-ray photoelectron spectroscopy using an Omicron Nanotechnology XPS system with a monochromatic $\text{Al K}\alpha$ radiation ($h\nu = 1,486.6 \text{ eV}$) of source voltage 15 kV and emission current of 20 mA . All scans were carried out at ultrahigh vacuum of $2 \times 10^{-10} \text{ mbar}$. Mass data of the product was analyzed by GC-MS analyzer equipped with 5975C inert MSD with Triple-Axis Detector and 7890A GC system.

2.2 Preparation of graphene- TiO_2 composite (RGO(5%)-T)

GO was synthesized via the modified Hummers method (25). 0.5 g of GO was dispersed in 100 mL of isopropanol by sonication for 2 hours to obtain a clear brown dispersion of graphene oxide. 3.5 mL of titanium isopropoxide was added into the dispersion and the mixture was stirred for 30 min at room temperature. Then 1 mL of distilled water was added dropwise under sonication and the mixture was kept

stirring for 24 hrs. The pale yellow sol was then transferred into a 500 mL Teflon-lined stainless steel autoclave and heated at 180°C for 24 h. The product was washed with distilled water several times and dried at 80°C .

2.3 Photocatalytic reaction

Photocatalytic reactions were carried out in an Oriol Arclamp system designed to produce uniform illumination. The light source was 150 W Xe ozone free lamp with average life of $1,500 \text{ h}$. A $420\text{--}630 \text{ nm}$ dichroic mirror (cold mirror) filter was used in order to get visible radiation, which gave an irradiance of 96.8 mW/cm^2 (150 W). Photo-oxidation reaction was carried out as follows. Benzyl amine in CH_3CN (0.1 mmol) was taken in a 100 mL beaker and 0.03 g of the catalyst was added to it. The suspension was stirred for about 20 min in the dark to achieve an adsorption/desorption equilibrium before placing under the lamp setup. Then the mixture was irradiated for 30 minutes. As a control, we also carried out the same reaction without the catalyst. The resultant reaction mixture was centrifuged and filtered using a Whatman filter paper and the product analysis was done by GC-MS analysis.

III. Results and Discussion

3.1 X-ray diffraction

The crystal structures of the prepared graphite oxide and the composite were identified by powder X-ray diffraction (XRD). Fig.1 shows the XRD pattern of graphite oxide synthesized by modified Hummer's method.

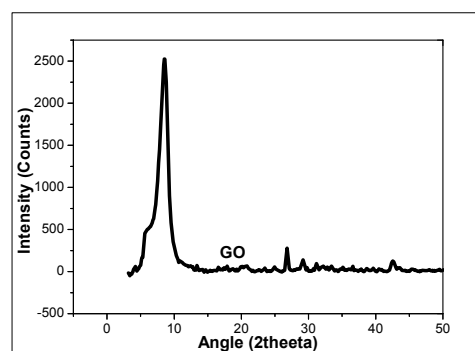


Fig. 1 XRD pattern of Graphite oxide

After oxidation, the graphitic peak at $\sim 26.5^\circ$ was disappeared and a new broad diffraction peak was observed at $2\theta = 8.572^\circ$ with an interlayer distance of 10.3 \AA corresponds to the GO. The disappearance of the graphitic peak ensures the oxidation of graphite into GO (26).

Fig.2 shows the XRD patterns of pristine titania and RGO(5%)-T. The peaks at 2θ value of 25.3° , 37.8° , 48.0° , 54.0° , 55.1° , 62.7° , 68.8° , 70.3° and 75.1° are indexed to (101), (004), (200), (105), (211), (204), (116), (220) and (215) crystal planes of anatase

TiO₂. The incorporation of graphene resulted in a lowering of intensity of anatase peaks. No diffraction peaks for carbon species are observed in the RGO(5%)-T composites. The main characteristic peak of graphene is at ~25°, so the peaks for graphene might be overlapped by the strong peak of anatase TiO₂ at 25.3°. The diffraction intensity of graphene is weak due to the lower mass ratio of graphene in the RGO(5%)-T composites (27).

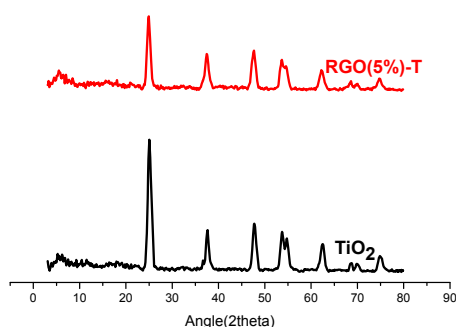


Fig. 2 XRD pattern of RGO(5%)-T and TiO₂

3.2 UV-VIS DRS Analysis

Fig. 3 shows the UV-Vis diffuse reflectance spectra (DRS) of pure TiO₂ and RGO(5%)-T nanocomposite. The addition of graphene improved the visible light absorption ability of RGO(5%)-T. Also, RGO(5%)-T nanocomposite showed a red shift in the absorption edge, indicating the narrowing of TiO₂ band gap. The band gap of the modified system was calculated to be around 2.21 eV, which is lower than that of bare TiO₂ (3.2 eV). The dark color of the RGO(5%)-T composite enhances the background absorption in the visible region. Moreover, the chemical bonding between titanium ions and oxygen groups of graphene also attributes to the visible light absorption (28).

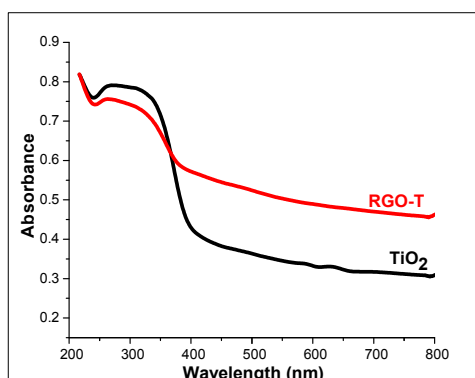


Fig. 3 UV-Vis diffuse reflectance Spectra of RGO(5%)-T and TiO₂

3.3 FTIR analysis

FTIR spectrum of the prepared GO material shows the bands at 1741 cm⁻¹ (C=O stretching vibrations from carbonyl and carboxylic groups), 1629 cm⁻¹ (O-H bending vibration from adsorbed H₂O), 1395 cm⁻¹ (C-OH stretching vibrations of COOH groups), 1235 cm⁻¹ (epoxy stretching vibration) and 1100 cm⁻¹ (alkoxy stretching peak), which provides evidence for the presence of different types of oxygen-containing functional groups such as -COOH, -C=O, -C-OH, and epoxy groups on the GO material. In the spectrum of RGO(5%)-T, the intensity of bands corresponding to -COOH, -C-OH and epoxy groups decreased significantly and some of them even disappeared, suggesting the removal of most of the groups caused by the redox reaction between Ti(III) precursor and GO and the subsequent hydrothermal treatment.

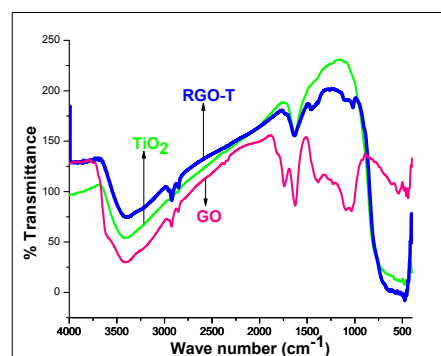


Fig. 4 FTIR spectra of TiO₂, RGO-T and GO
 The bands below 1000 cm⁻¹ can be ascribed to Ti-O-Ti stretching vibration (29).

3.4 XPS Analysis

Complete electronic structure of as-prepared graphene oxide and the composite were identified from XPS measurements.

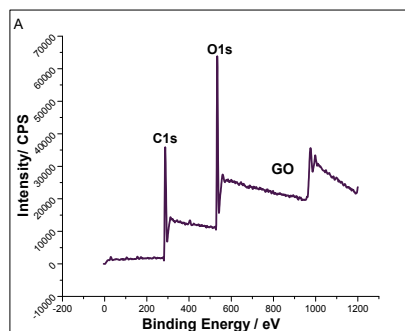


Fig. 5 Survey scan of GO

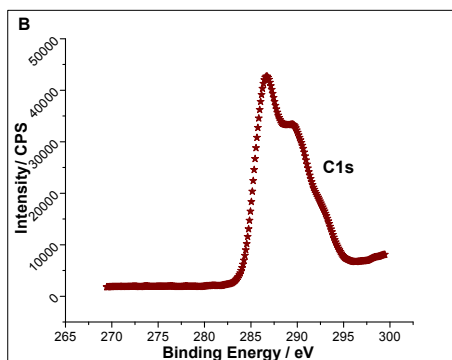


Fig.6 C1s core level spectrum of GO

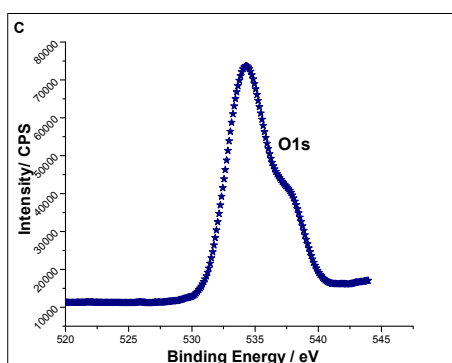


Fig. 7 O1s core level Spectrum of Graphite oxide

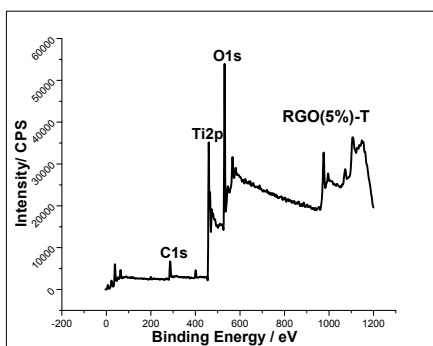


Fig. 8 Survey scan of RGO(5%)-T

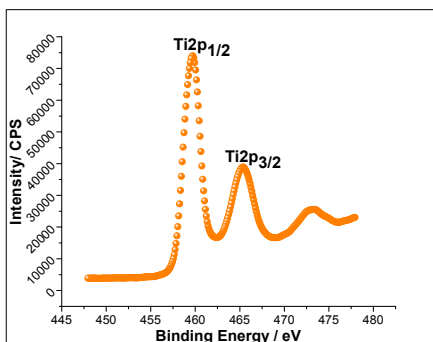


Fig. 9 Ti2P core level spectrum of RGO(5%)-T

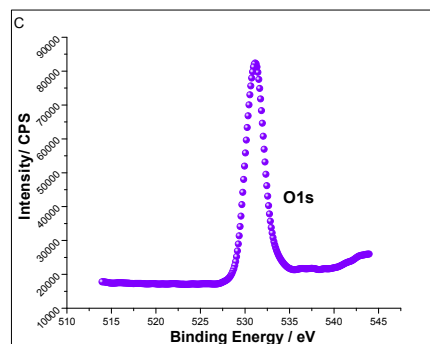


Fig. 10 O1s Core level spectrum of RGO(5%)-T

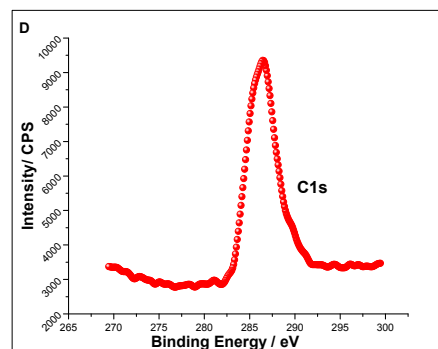


Fig. 11 C1s core level Spectrum of RGO(5%)-T

XPS spectrum of GO shows two peaks around binding energies of 286.6eV and 289.5eV can be assigned to the C=O and O=C-OH functional groups respectively. Two major peaks observed at 459.7eV and 465.4eV corresponding to the Ti2p_{3/2} and Ti2p_{1/2} levels conformed Ti⁴⁺ species with stable Ti-O bond in the RGO(5%)-T system. The main peak centered at about 285 eV in GO sample is originated from the graphitic sp² carbon atoms. The two peaks located at 286.4 eV and 289.7 eV are due to carbon atoms connecting with oxygenate groups, such as C-O and O=C-OH respectively. The lower intensity peaks due to oxygenate groups suggest a considerable deoxygenation and the formation of RGO. The XPS results show that most oxygenate groups was removed during the redox reactions. The peaks around 529.9 eV and 531.1eV are ascribed to the bulk O²⁻ from TiO₂ and -OH adsorbed on the surface of RGO-T nanocomposite respectively. The O1s peak at 533.9 eV can be ascribed to C-O bond. The presence of peak having lower intensity centered at ~460.1eV can be ascribed to Ti-C bonding.

3.5 SEM-Analysis

SEM micrographs were performed to determine the morphology of samples. The figure shows (Fig. 12) the distribution of titania particles on graphene sheets. The prepared sample consists of nearly spherical particles with some degree of aggregation. The shapeless structures in the image are

mainly due to aggregation and that may happened during hydrothermal synthesis.

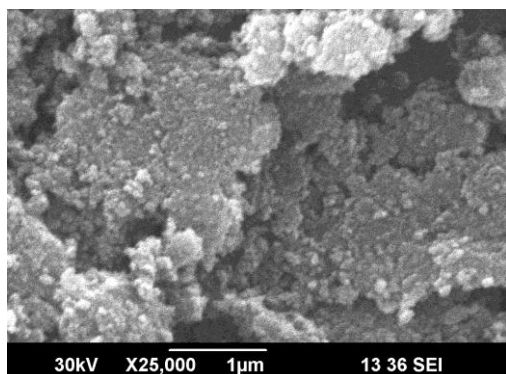


Fig. 12 SEM image of RGO(5%)-T

3.6 TEM Analysis

TEM showed irregularly shaped structures due to the agglomeration of particles.

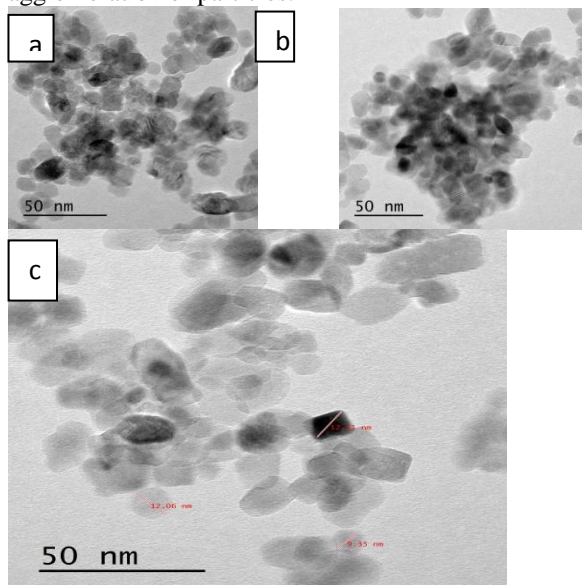


Fig. 13 TEM images of RGO(5%)-T

Fig. 13 shows the TEM images of RGO(5%)-T. Distribution of spherical TiO_2 nanoparticles can be clearly observed from the TEM images. Particles having size ranging from 9 nm to 15 nm was observed from the image.

3.7 Photocatalytic activity studies

The photocatalytic activity of the prepared RGO(5%)-T composite was evaluated by monitoring the photo-oxidation of benzyl amine to corresponding imine. The reaction was monitored by GC-MS analysis. The substrate used was not active under visible light irradiation because its absorption maximum is purely in the UV region. So the possibility for sensitization of composite by the substrate is not possible. Irradiation of the suspension

by visible light results initial excitation from composite, which drives the reaction effectively. Light and molecular oxygen are the two major driving forces in photo-oxidation reactions. In this reaction, molecular oxygen was not added to the reaction mixture externally. The electrons generated in the conduction band due to irradiation could easily be captured by molecular oxygen adsorbed on the catalyst surface to form some reactive oxygen species, which in turn react with the substrate molecules. The optimum amount of catalyst was chosen to be 0.3 g since a lower amount gave a marginal yield and a higher amount made the suspension too thick for the light to transmit and resulted in a lower yield. N-benzylidene-1-phenylmethanamine was the only product formed after 30 minutes of the reaction, with almost 100% selectivity which is indicated by the single peak in the chromatogram. The mass spectrum further confirms the formation of N-benzylidene-1-phenylmethanamine ($m/z = 195$). Nobody has reported this particular transformation in such a short duration of time, which showed the efficiency of our prepared system. No peak corresponding to benzyl amine was recovered in the chromatogram after 30 minutes confirmed the complete conversion of the substrate. Formation of imine from amine follows a two-step mechanism 1) a selective oxygenation of benzyl amine into benzaldehyde 2) nucleophilic addition of benzaldehyde by benzyl amine to imine. The incorporation of graphene into titania resulted an increased adsorption of the reactants which in turn enhanced the rate of reaction. It also facilitated the reaction to proceed under visible light. Fig. 14 represents the GCMS results of reactant and product.

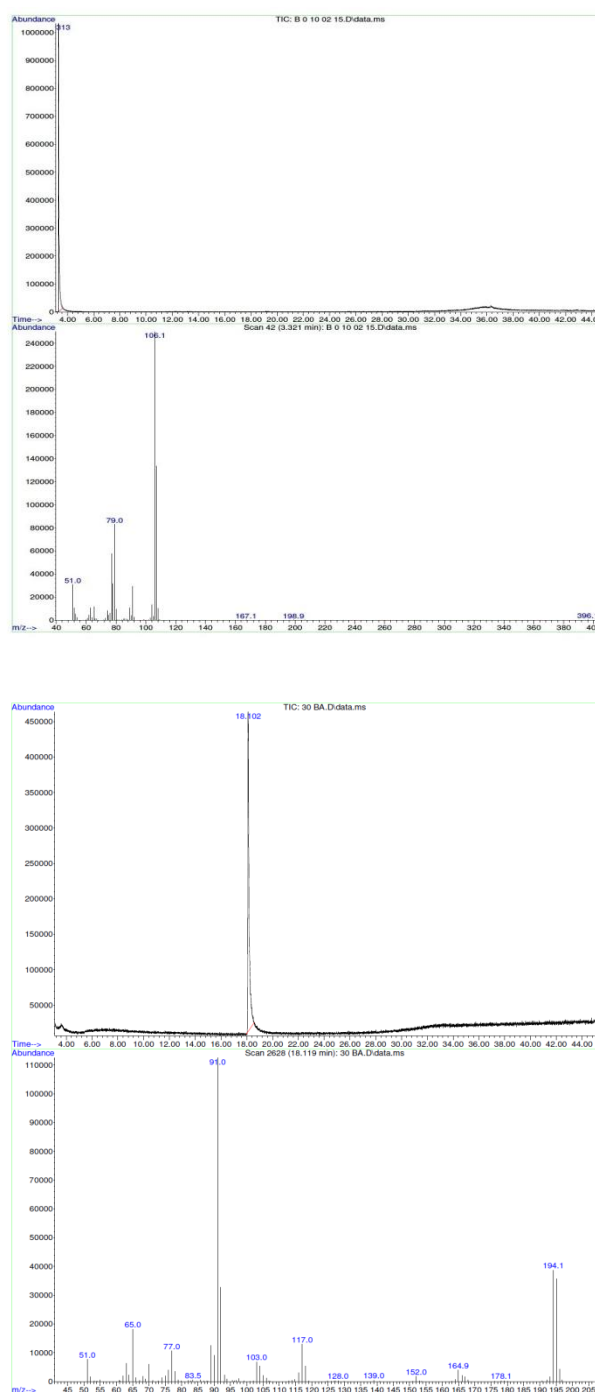


Fig. 14 GC-MS Results of the reactant and product.

IV. CONCLUSION

Semiconductor mediated photocatalysis can be considered as an effective means for selective organic transformations. Cost effective, recyclable and environmentally benign reduced graphene oxide-titania composite was synthesized by hydrothermal method which showed an extended light absorption in the visible region. The composite successfully converted benzyl amine to N-benzylidene-1-

phenylmethanamine in a short period of time with almost 100% selectivity. The enhanced photocatalytic activity might be due to the incorporation of highly conducting 2-dimensional graphene onto titania which lowered the electron-hole recombination and also resulted the increased adsorption of the organic compounds by π - π interaction. The product analysis was carried out by GC-MS analysis.

References

- [1] F. Fresno, R. Portela, S. Suarez, J. M. Coronado, *J. Mater. Chem. A*, 2 (2014), 2863-2884.
- [2] K. Nakata, T. Ochiai, T. Murakami, A. Fujishima, *Electrochimica Acta*, 84 (2012) 103-111.
- [3] Y. Shiraishi, T. Hirai, *J. Photochem. Photobiol. C: Photochem. Rev.*, 9 (2008) 157-170.
- [4] C. Karunakaran, S. Karuthapandian, *Egypt. J. Basic and Appl. Sci.*, 2 (2015) 32-38.
- [5] M. Fagnoni, D. Donbi, D. Ravelli, A. Albini, *Chem. Rev.*, 107 (2007) 2725-2756.
- [6] Y. Shiraishi, T. Hirai, *J. Japan Petroleum Institute*, 55(5) (2012) 287-298.
- [7] R. K. Nath, M. F.M. Zain, A. A. H. Kadhum, *J. Appl. Sci. Res.*, 8(8) (2012) 4147-4155.
- [8] C. Chen, W. Ma, J. Zhao, *4206 Chem. Soc. Rev.*, 39(2010) 4206-4219.
- [9] Y. Ni, W. Wang, W. Huang, C. Lu, Z. Xu, *J. Col. Inter. Sci.*, 428 (2014) 162-169.
- [10] A. L. Linsebigler, G. Lu, J. T. Yates, Jr, *Chem. Rev.*, 95(1995)735-758.
- [11] TiO₂ Nanostructures: Recent Physical Chemistry Advances Editorial pubs.acs.org/JPCCE © 2012 editorial *J. Phys. Chem. C*, 116(2012) 11849-11851.
- [12] M. R. Hoffmann, S. T. Martin, W. Choi, D. W. Bahnemannt, *Chem. Rev.*, 95(1) (1995) 69-96.
- [13] W. Geng, H. Liub, X. Yao, *Phys. Chem. Chem. Phys.*, 15 (2013) 6025-6033.
- [14] Z. Wang, Y. Liu, B. Huang, Y. Dai, Z. Lou, G. Wang, X. Zhanga, X. Qina, *Phys. Chem. Chem. Phys.*, 16 (2014) 2758-2774.
- [15] A. B. Djuricic, Y. H. Leunga, A. M. Ching, *Mater. Horiz.*, 1(2014) 400-410.
- [16] S. Morales, L. M. Pastrana, J. L. Figueiredo, J. L. Faria, A. M. T. Silva, *Environ. Sci. Pollut. Res.*, 19 (2012) 3676-3687.
- [17] A. K. Geim, K. S. Novoselov, *Nature Mat.*, 6 (2007) 183-191.
- [18] K. S. Novoselov, *Angew. Chem. Int. Ed.*, 50 (2011) 6986 - 7002.
- [19] K. P. Loh, Q. Bao, P. K. Ang, J. Yang, *J. Mater. Chem.*, 20 (2010) 2277-2289.
- [20] J. S. Lee, K. H. You, C. B. Park, *Adv. Mater.*, 24 (2012) 1084-1088.

- [21] Q. Xiang, J. Yu, M. Jaroniec, *Chem. Soc. Rev.*, 43 (2011) 473-486.
- [22] N. Li, X. Lang, W. Ma, H. Ji, C. Chen, J. Zhao, *Chem. Commun.*, 49 (2013) 5034-5036.
- [23] X. Lang, X. Chen, J. Zhao, *Chem. Soc. Rev.*, 43 (2014) 473-486.
- [24] X. Lang, W. Ma, Y. Zhao, C. Chen, H. Ji, J. Zhao, *Chem. Eur. J.*, 18 (2012) 2624 – 2631.
- [25] D. C. Marcano, D. V. Kosynkin, J. M. Berlin, A. Sinitskii, Z. Sun, A. Slesarev, L. B. Alemany, W. Lu, J. M. Tour, *ACS NANO* 4(2010), 4806–4814.
- [26] K. Krishnamoorthy, R. Mohan, S. J. Kim, *Appl. Phy. Lett.*, 98(2011) 244101.
- [27] P. Cheng, Z. Yang, Hong Wanga, W. Cheng, M. Chen, W. Shangguan, G. Ding, *Int. J. hydrogen energy*, 37 (2012) 2224-2230.
- [28] X. Zhang, Y. Sun, X. Cui, Z. Jiang, *Int. J. Hydrogen Energy*, 37 (2012) 811 -815.
- [29] Z. Y. Fei, X. Yun, S. Z. Yu, Z. H. Ye, T. R. Ting, H. C. Liang, L. Z. Min, *Science China Press and Springer-Verlag Berlin Heidelberg*, 55 (2012) 1294–1302.